Materials Science for Energy Technologies 3 (2020) 508–514

Contents lists available at ScienceDirect

Materials Science for Energy Technologies

journal homepage: www.keaipublishing.com/en/journals/materials-science-for-energy-technologies

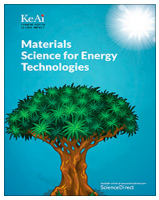

# A sugar derived carbon-red phosphorus composite for oxygen evolution reaction and supercapacitor activities

Mohd. Khalid [a,*], Ana M.B. Honorato [b], André A. Pasa [c], Hamilton Varela [a,*]

[a] Institute of Chemistry of São Carlos, University of São Paulo, PO Box 780, 13560-970 São Carlos, SP, Brazil
[b] Department of Materials Engineering, Federal University of São Carlos, Washington Luiz Rd, Km 235, BR13565905 São Carlos, SP, Brazil
[c] Laboratório de Filmes Finos e Superfícies, Departamento de Fisica, Universidade Federal de Santa Catarina 88040-900 Florianopolis, Brazil

ARTICLE INFO

*Article history:*
Received 21 February 2020
Revised 30 April 2020
Accepted 1 May 2020
Available online 25 May 2020

*Keywords:*
Sugar
Red phosphorous
Composite
OER
Supercapacitor

ABSTRACT

The development of low-cost and highly active electrode material is essential for the growth of renewable energy conversion and storage technologies. In this work, a composite of carbon-red phosphorous has been synthesized using a simple chemical reaction of sugar with sulfuric acid in presence of red phosphorous followed by carbonization. The as-prepared carbon-red phosphorous composite displays oxygen evolution reaction (OER) activity with an overpotential of 1.69 V vs. RHE to achieve 10 mA $cm^{-2}$ current density compared to pristine carbon (1.81 V vs. RHE). Moreover, a symmetrical supercapacitor has been constructed, which delivers a specific capacitance of 105.8 F $g^{-1}$ and retains 100% of its initial capacitance after repeating 3000 voltammogram cycles. This simple and low-cost preparation of carbon-red phosphorous composite from sugar can open up exciting opportunities for energy conversion and storage applications.

## 1. Introduction

Carbons have attracted great deal of interest in electrochemical energy conversion and storage technologies, such as fuel cells, metal-air batteries, and supercapacitors [1]. Currently, the expensive $RuO_2$ and $IrO_2$ are regarded the best electrocatalysts for OER. However, unaffordable cost and scarcity have limited their use for commercial purpose [2]. On the other hand, non-noble metal-based catalysts (e.g.; Fe, Co, and Ni) are insufficient as they usually show inferior catalytic activity and high susceptibility to be oxidized in air [3,4]. To this perspective, the development of low cost and highly active catalyst materials has been imperative. Over the past decades, carbon materials have become a hot topic in energy conversion and storage applications, owing to their unique physicochemical properties, excellent electrical/thermal conductivities, and tunable surface chemistry [5–7].

Recently, our group has reported a general potentiodynamic strategy for the incorporation of red phosphorus and sulfur nanodots into reduced graphene oxide sheets. The as-synthesized composite materials simultaneously served for both supercapacitor and hydrogen evolution activities [8]. In another work, we prepared nitrogen and sulfur co-doped carbon uniformly decorated with $Co_3O_4$, which demonstrated excellent OER activity by showing an onset potential of 1.41 V vs. RHE in alkaline medium [9]. The new allotropes of carbon such as graphdiyne and graphyne have also been proven as excellent electrocatalysts [10–13],[14]. Kong et al. predicted B-doped γ-graphyne as an efficient material for OER by calculating the free energy changes of OER [15].

Recently, J. S. Yu et al. have synthesized doped carbon from human urine for oxygen reduction reaction and supercapacitor applications [16,17]. The preparation of above-mentioned carbon material is a complex and requires multistep process. Therefore, to develop a simple route for the fabrication of carbon-based material at large scale is of great importance [18,19]. Toward this end, carbonization of biomass is a great choice because of their easy availability, low cost, chemical stability, and good electrical conductivity. The biomass sugar derived carbon has seldom been used as electroactive material, to our knowledge. Sugar also known as 'cane sugar' is basically a sucrose, often used in our daily life, contains C, H, and O elements and can produce carbon material upon pyrolysis. In this work, the composite of carbon-red phosphorous has been prepared from the mixture of sugar powder and red phosphorus by a facile chemical reaction with sulfuric acid followed by pyrolysis. The sulfuric acid acts as a dehydrating agent and convert sugar powder into a foam like carbon material. The resulted

* Corresponding authors.
*E-mail addresses:* mkansarister@gmail.com (Mohd. Khalid), hamiltonvarela@usp.br (H. Varela).

Peer review under responsibility of KeAi Communications Co., Ltd.

https://doi.org/10.1016/j.mset.2020.05.002

composite displayed reasonably good electrochemical properties for both oxygen evolution reaction and supercapacitor. Such a newly developed strategy for the development of carbon-based electroactive material from sugar powder would certainly pave the way for next generation renewable energy technologies.

## 2. Experimental detail

### 2.1. Chemical reagents and materials

The powder of refined sugar (Brand UniÕn) with particle size of ~0.25 mm was purchased from supermarket. Red phosphorous, ruthenium oxide ($RuO_2$, 99.9%), and sulfuric acid ($H_2SO_4$, 97%) were purchased from Sigma-Aldrich and used as received without further purification. Nafion (Aldrich, 5 wt%) was used in ethanol. The deionized water was used from Milli-Q Advantage A10 (Merck Millipore, USA) with a resistivity of 18.25 MΩ $cm^{-1}$.

### 2.2. Preparation of the materials

In a typical synthesis, 10 g sugar powder and 1 g red phosphorous were manually ground with the help of agate mortar. The mixture was then transferred into a glass beaker of 500 mL. Afterward, the mixture was reacted with 10 mL of concentrated sulfuric acid in a fume hood under atmospheric condition. The foam like carbon was obtained and washed with copious amount of distilled water until the acid is completely removed. The as-prepared carbon foam was carbonized in a tubular furnace under argon atmosphere at 900 °C for 3 h with ramp rate of 2 °C $min^{-1}$.

### 2.3. Material characterizations

Oxford scanning electron microscopy (LEO, Model 440) and transmission electron microscopy (JEM2100 $LaB_6$ 200 kV) were used to analyze morphological structure of materials. For TEM analysis, a little amount of material was dispersed in isopropyl alcohol and ultrasonicated for 10 min, then a drop of solution was casted on carbon-film copper grids (EMS, 400 mesh). The X-ray diffraction patterns were recorded using a Bruker D8-advance X-ray powder diffractometer with Cu Kα radiation source (λ = 1.5 4 Å). Raman spectra were collected on a Jobin-Yvon LabRam HR 800 Raman spectroscope equipment with a 500 nm laser source. X-ray photoelectron spectroscopy (XPS, PHI-5300ESCA, PerkinElmer was used to analyze the materials.

### 2.4. Electrochemical measurements

The electrochemical measurements were investigated by Metrohm Autolab electrochemical workstation. The OER experiments were carried out in a standard three-electrode cell configuration using $N_2$-saturated 1 M KOH electrolyte under the scan rate of 5 mV $s^{-1}$ at room temperature of *ca.* 25 °C. The Hg/HgO (1 M KOH filling solution) and Pt plate (1 $cm^2$) were used as reference and counter electrodes, respectively. For the ink preparation of catalyst, 2 mg material was dispersed in 400 μL of isopropyl alcohol and 40 μL of 5 wt% Nafion solution and then ultrasonicated for 30 min to obtain a homogeneous mixing of catalyst. Same procedure was applied to prepare the ink of commercial $RuO_2$ catalyst for comparison. Subsequently, a predetermined volume of the catalyst dispersion (5 μL) was carefully casted onto the polished glassy carbon rotating disk electrode (0.0314 $cm^2$) and dried under ambient condition. The average catalyst loading amount was approximately ~0.025 mg. All the potentials were calibrated and converted to reversible hydrogen electrode (RHE) using equation $E_{vs\ RHE} = E_{vs\ Hg/HgO} + 0.095 + 0.059pH$. For the electrode fabrication, the precleaned carbon cloth piece (1.5 cm width and 3 cm length) was dipped several times in the ink of active material (2 mg material + 400 μL of isopropyl alcohol +40 μL of 5 wt% Nafion solution) and dried under nitrogen stream for 10 min. The loading of material on electrode was ~0.3 mg. For the construction of symmetric supercapacitor, two electrodes with same shape and size were dipped into the electrolyte solution (1 M $H_2SO_4$) with the assistance of platinum wires, using both as positive and negative electrodes. The specific capacitance, specific energy, and specific power were calculated by the following equations.

$$C_{cell} = I/(dv/dt) \quad (1)$$

where, $C_{cell}$ is the capacitance of the supercapacitor cell, $I$ is the constant discharge specific current (A), and $dv/dt$ is the slop of discharge curve.

$$C_{sp} = 4C_{cell}/M_{two-electrode} \quad (2)$$

where, $C_{sp}$ is the specific capacitance of the active electrode and $M$ is the mass of two electrodes.

$$E = \frac{1}{8}CV^2 \quad (3)$$

where, $E$ is the specific energy, $C$ is the specific capacitance ($C_{sp}$) of the electrode, and $V$ is the potential window.

$$P = \frac{E}{t_{dischargetime}} \quad (4)$$

where, $P$ is the specific power and $t$ is the discharge time in seconds.

## 3. Results and discussion

The sugar powder and red phosphorous were mixed together in predetermined amounts and then the mixture was ignited by concentrated sulfuric acid resulting in a foam like carbon material, as shown in Scheme 1. During the reaction, sulfuric acid acted as a dehydrating agent and blown the sugar powder into a piece of carbon foam in few seconds by liberating carbon dioxide gas. The carbon foam was then subjected to pyrolysis in a tube furnace at 900 °C for 3 h under argon atmosphere. During pyrolysis, the red phosphorous sublimed and introduced into carbon matrix thereby forming a composite of carbon-red phosphorous (CP). Pristine carbon was prepared following the same procedure above but without adding red phosphorous powder.

The typical scanning electron microscopy (SEM) images of pristine carbon and CP composite (Fig. 1a, b) showed stalked layered type carbon structure with several micrometer sizes. The CP composite demonstrated rough surface of carbon, while pristine carbon shows smooth surface of carbon. The high-resolution transmission electron microscopy (HRTEM) image of CP composite (Fig. 1c) presented a wrinkled layered-structure of carbon, this could be due to the irregular stalking of multiple layers of carbon. Fig. 1d, shows the selected area electron diffraction pattern (SAED), where two blurred rings can be observed, suggesting the graphitic reflection of the carbon. The corresponding energy dispersive X-ray (EDX) elemental mapping images show the uniform distribution of P (red) and O (purple) elements all over the carbon (green) layer, which can afford numerous active sites for catalysis. The compositional data was obtained from EDX analysis and found to be 80.5, 12.8, and 6.7%, for C, O, and P, respectively. In the XRD pattern (Fig. 1e) of CP composite, there are two broad peaks at 23.7° (0 0 2) and 44° (10), indicating that sugar powder has been completely converted into carbon material [20,21]. The diffraction plan (0 0 2) can be ascribed to the parallel stalking of layered carbon and (10) is typically from graphitic carbon [22]. On the other hand, the XRD pattern of carbon foam (without carbonized) shows no peak, meaning that the reaction of sugar with sulfuric acid only produced ash (partially burnt sugar).

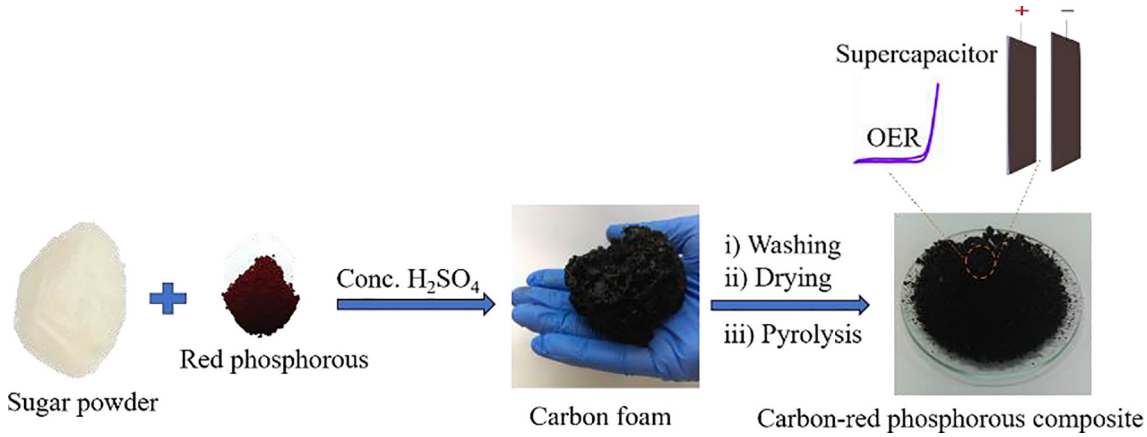


**Scheme 1.** illustration for the preparation of carbon-red phosphorous composite.

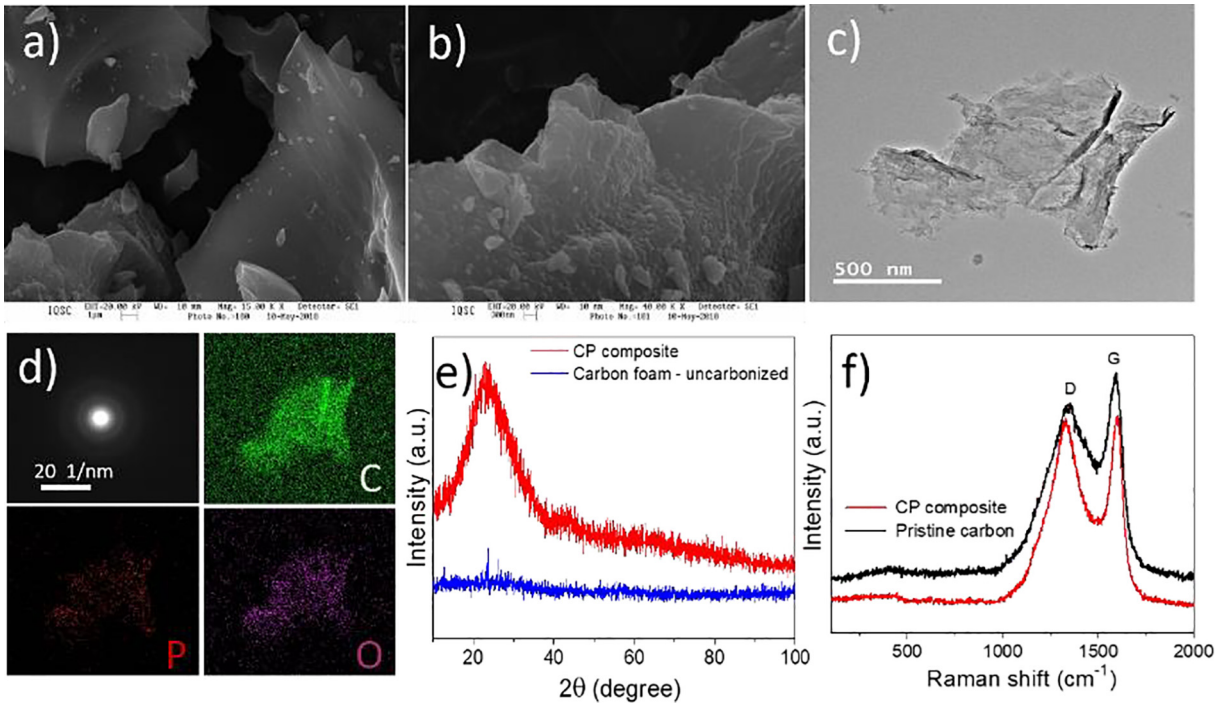


**Fig. 1.** a, b) SEM images of pristine carbon and CP composite, respectively, c) HRTEM image of CP composite, d) SAED pattern and corresponding elemental mapping images of C, O, and P, e) XRD patterns of CP composite and uncarbonized carbon foam, and f) Raman spectra.

The Raman spectra of CP composite and pristine carbon (Fig. 1f) show two sharp peaks at 1575 $cm^{-1}$ (G band) which is of the characteristic scattering peak of graphitic carbon and the peak at 1350 $cm^{-1}$ (D band) corresponding to the lattice defects, disorder arrangement and low symmetry carbon structure of graphite [23]. The degree of defects in the samples can be evaluated by the intensity ratio of D and G bands. The intensity ratios ($I_D/I_G$) for CP composite and pristine carbon were calculated to be 0.97 and 0.88, respectively. The high value of ID/IG (0.97) for composite CP is reflecting a higher defect concentration in composite material that can provide more active sites for the electrode enhancing electrochemical performance.

The high-resolution X-ray photoelectron spectroscopy (XPS) spectra of C 1s, P 2p, and O 1s were measured to analyze the chemical environment of composite CP. Fig. 2a represents the XPS survey spectrum, that confirms the presence of P and O elements in the carbon. Fig. 2b shows the high resolution XPS spectrum of C 1s corresponding to "$sp^2$ C" (284.4 eV), "$sp^3$ C" (285.3 eV), and "C-O" (287.8 eV) peaks [24,25]. The XPS spectrum of P 2p (Fig. 2c) displays two peaks at 133.5 and 134.3 eV, which attribute to the spin-orbit splitting (doublet) of $2p_{3/2}$ and $2p_{1/2}$ components of P-O bond [26]. This implies that the P is not chemically bonded with C atom, rather than both components are electrostatically interacted each other by making a composite of carbon and red phosphorous particles. The XPS spectrum of O 1s (Fig. 2d) shows the peaks at 532.2 and 533.6 eV, which were assigned to C-O, and P-O bonds respectively.

### 3.1. OER study of carbon-red phosphorous composite

The OER activity of the samples were conducted under LSV measurement with $N_2$-saturated 1 M KOH aqueous electrolyte at rotation speed of 1000 rpm. As shown in Fig. 3a, the CP composite displayed reasonably good OER activity by showing an overpotential of 1.69 V vs. RHE to achieve 10 mA $cm^{-2}$ current density compared to pristine carbon (1.81 V vs. RHE). As expected, the

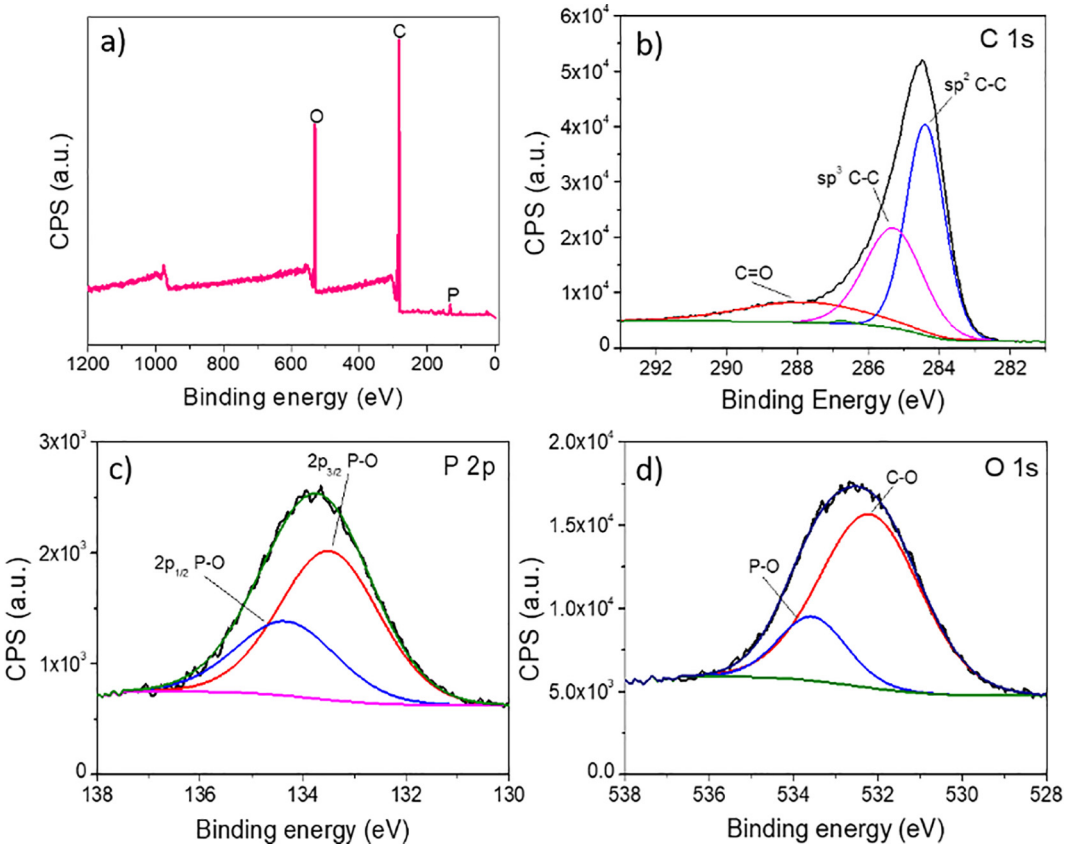


**Fig. 2.** a) XPS survey spectrum of CP composite, b) XPS of C 1 s, c) XPS of P 2p, and d) XPS of O 1 s.

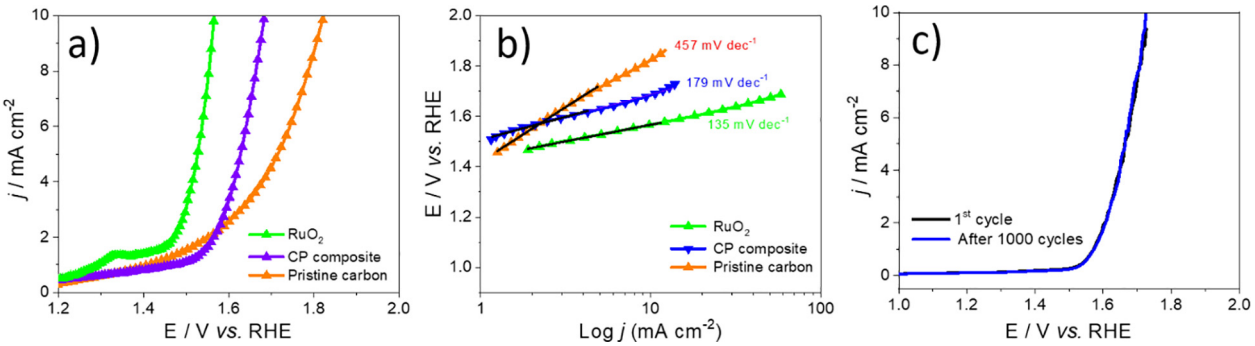


**Fig. 3.** OER analysis. a) LSV profiles of CP composite, pristine carbon, and $RuO_2$ at 5 mV $s^{-1}$ in $N_2$-saturated 1 M KOH solution, b) Corresponding Tafel plot, and c) LSV profile of CP composite before and after 1000 CV cycles.

benchmark $RuO_2$ showed better performance by achieving 10 mA $cm^{-2}$ current density at lowest overpotential of 1.54 V vs. RHE. The OER activity of CP composite was found comparable to that of carbon based electrocatalysts as reported by other groups, as represented in Table 1 [5],[27–35].

Tafel plot which was derived from the LSV polarization curves, showed the Tafel slope values of ~135, 179, and 457 mV $dec^{-1}$ for $RuO_2$, CP composite, and pristine carbon, respectively (Fig. 3b). The low Tafel slope of 179 mV $dec^{-1}$ for CP composite may represent the Heyrovsky step for the kinetics of OER compared to pristine carbon. This clearly indicates that there is an emergence of synergistic effect between carbon and red phosphorous. The relatively large Tafel slope values of the samples might be due to the involvement of some side reactions during OER [36,37]. The OER stability of the CP composite was observed by similar LSV curves measured before and after 1000 CV cycles between the potential rang of 1.3 to 1.6 V vs RHE at scan rate of 5 mV $s^{-1}$ (Fig. 3c). These results indicate that the carbon-red phosphorous composite derived from sugar could be a promising low-cost electrocatalyst for oxygen evolution reaction.

### *3.2. Supercapacitor study of sugar derived carbon-red phosphorous composite*

To evaluate the supercapacitor performance of the as-prepared composite material, a symmetrical two-electrode cell was assembled using the same shape and size as positive and negative electrodes. Where negative electrode served as both counter and reference electrode and positive electrode served as working electrode. The electrochemical capacitor performance of the assembled cell was tested in 1 M $H_2SO_4$ electrolyte solution. The CV curves of CP composite show the increment in current with increasing scan rates from 10 to 200 mV $s^{-1}$ suggesting the high rate capability of

**Table 1**
Comparison of OER performance of CP composite with some lately reported carbon-based materials.

| Electrocatalysts | Electrolyte | Potential (V) at 10 mA $cm^{-2}$ | Tafel slop value (mV $dec^{-1}$) | Ref. |
|---|---|---|---|---|
| CP composite | 1 M KOH | 1.69 | 179 | This work |
| N-doped G/CNTs hybrids | 0.1 M KOH | 1.63 | 83 | [27], |
| g-$C_3N_4$/G | 0.1 M KOH | 1.81 | 68.5 | [28], |
| N, O, P-tri doped porous carbon | 1 M KOH | 1.63 | 84 | [29], |
| N, S co-doped G | 0.1 M KOH | 1.65 | 59 | [30], |
| N, O co-doped carbon hydrogel film | 0.1 M KOH | 1.63 | 141 | [31], |
| N, P co-dopedgraphene/carbonnano-sheets | 0.1 M KOH | 1.57 | 70 | [32], |
| Oxidized carbono cloth | 0.1 M KOH | 1.72 | 82 | [33], |
| B doped CNTs | 1 M KOH | 1.83 | – | [34], |
| N doped graphite | 0.1 M KOH | 1.61 | – | [5], |
| N, S co-doped graphitic sheets | 0.1 M KOH | 1.60 | 71 | [35], |

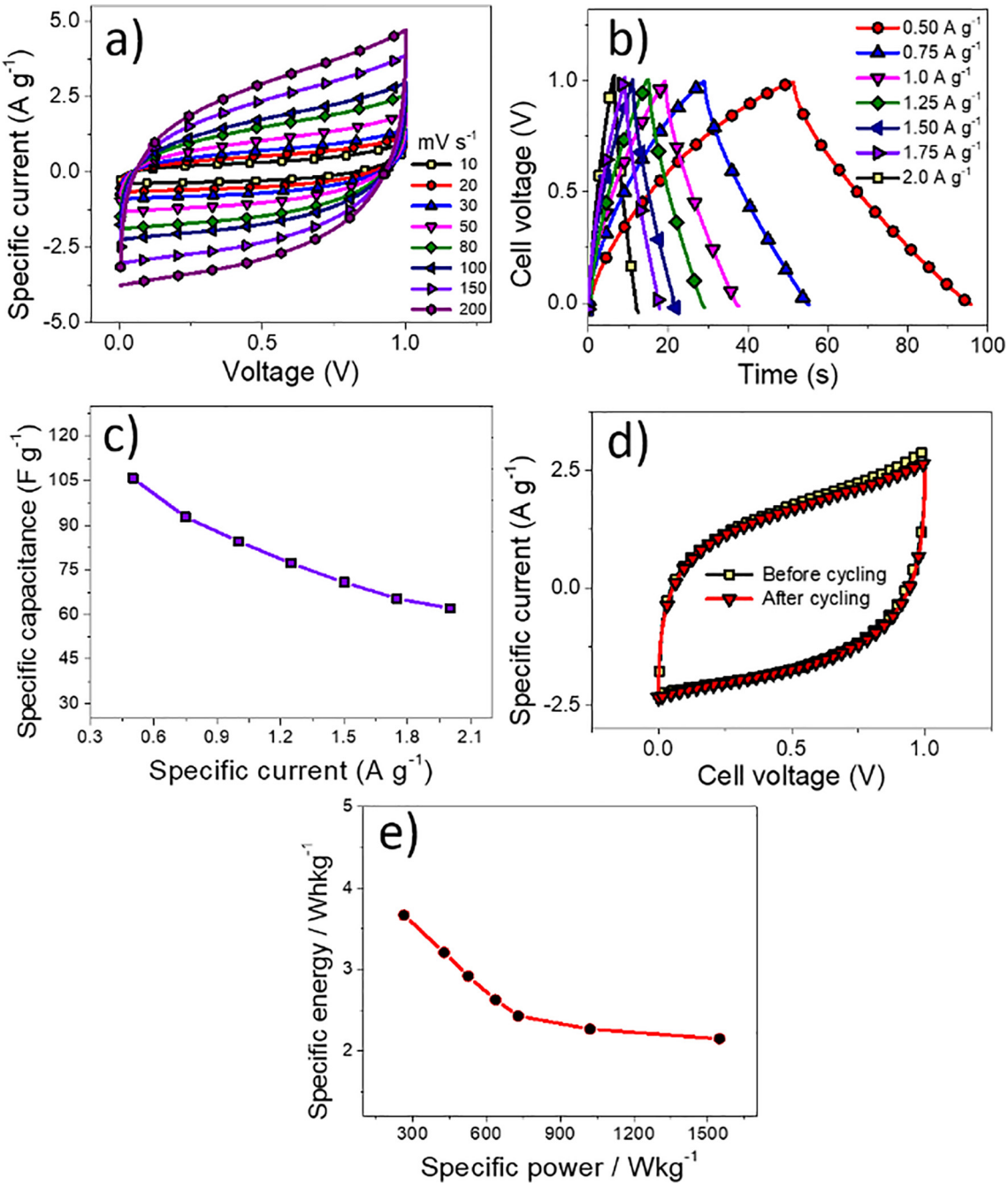


**Fig. 4.** Symmetric supercapacitor study of CP composite. a) CV curves at different scan rates, b) GCD curves at different specific currents, c) Plot of specific capacitance versus specific current, d) CV curves before and after 3000 CV cycles at 100 mV $s^{-1}$, and e) Plot for specific energy versus specific power.

the electrode material (Fig. 4a). The galvanostatic charge-discharge (GCD) profile show the quasi-linear shape of the curves further indicating a good capacitive characteristic of the electrode material in symmetric two electrode cell (Fig. 4b). The specific capacitance of the electrode was calculated to be 105.8F $g^{-1}$ at the specific current of 0.5 A $g^{-1}$. This was retained up to ~42% when specific current increased to 2 A $g^{-1}$, as shown in Fig. 4c. The cyclic performance of the symmetric supercapacitor was tested under a high scan rate of 100 mV $s^{-1}$ for consecutive 3000 CV cycles. The symmetric supercapacitor exhibited virtually no capacitance loss, as shown in Fig. 4d. This implies that the composite material has good electrochemical stability. For the practical application, determining the energy and power densities are the most important factors for full cell supercapacitors [38,39]. According to the Ragone plot as shown in Fig. 4e, the symmetric supercapacitor delivered the specific power of 264 $Wkg^{-1}$ at the specific energy of 3.67 Wh $kg^{-1}$. These results indicate that the sugar derived carbon-red phosphorous composite is a promising material for both energy conversion and storage applications.

## 4. Conclusions

A carbon-red phosphorous composite was successfully derived from sugar powder using a simple one step chemical reaction with sulfuric acid followed by carbonization. The as-prepared composite showed reasonably good OER activity by achieving a 10 mA $cm^{-2}$ current density at an overpotential of 1.69 V vs. RHE. The as-prepared composite showed the specific capacitance of 105.8 F $g^{-1}$ and excellent electrochemical stability in acid medium. Additionally, the symmetric supercapacitor cell demonstrated a specific power of 264 $Wkg^{-1}$, while maintaining the specific energy of 3.67 Wh $kg^{-1}$. Thus, this work provides a sustainable and cost-effective approach for synthesizing carbon-red phosphorous composite material for both energy conversion and storage applications.

## CRediT authorship contribution statement

**Mohd. Khalid:** Conceptualization, Data curation, Formal analysis, Funding acquisition, Methodology, Project administration, Writing – original draft. **Ana M.B. Honorato:** Data curation, Investigation, Visualization, Writing – review & editing. **André A. Pasa:** Validation, Visualization, Writing – review & editing. **Hamilton Varela:** Resources, Software, Supervision, Validation, Visualization, Writing – review & editing..

## Declaration of Competing Interest

The authors declare that they have no known competing financial interests or personal relationships that could have appeared to influence the work reported in this paper.

## Acknowledgements

Authors thank to the São Paulo Research Foundation (FAPESP) for financial support under ongoing projects of M.K. (Grant No. 2017/00433-5), and H.V. (Grant No. 2013/16930-7). H.V. also would like to acknowledge Conselho Nacional de Desenvolvimento Cientifico e Tecnologico (CNPq) for financial support under Grant no. 306060/2017-5 (Brasil). This study was also financed in part by the Coordenação de Aperfeiçoamento de Pessoal de Nível Superior – Brasil (CAPES) – Finance Code 001. The authors also thank Dr. Miguel Boratto from LFFS/UFSC for assisting with the evaluation of XPS data.

## References

[1] S. Chena, L. Zhao, J. Ma, Y. Wang, L. Dai, J. Zhang, Edge-doping modulation of N, P-codoped porous carbon spheres for high performance rechargeable Zn-air batteries, Nano Energy 60 (2019) 536–544.
[2] M.K. Debe, Electrocatalyst approaches and challenges for automotive fuel cell, Nature 486 (2012) 43–51.
[3] J. Ding, S. Ji, H. wang, H. Gai, F. Liu, V. Linkov, R. Wang, Mesoporous nickel-sulfide/nickel/N-doped carbon as HER and OER bifunctional electrocatalyst for water electrolysis, Int. J. Hydr. Enr. 44 (2019) 2832–2840.
[4] S. Chakrabarty, A. Mukherjee, W.-N. Su, S. Basu, Improved bi-functional ORR and OER catalytic activity of reduced graphene oxide supported $ZnCo_2O_4$, Int. J. Hydr. Enr. 44 (2019) 1565–1578.
[5] Y. Zhao, R. Nakamura, K. Kamiya, S. Nakanishi, K. Hashimoto, Nitrogen-doped carbon nanomaterials as non-metal electrocatalysts for water oxidation, Nat. Comm. 4 (2013) 2390.
[6] Y. Jiao, Y. Zheng, M. Jaroniec, S.Z. Qiao, Origin of the electrocatalytic oxygen reduction activity of graphene-based catalysts: a roadmap to achieve the best performance, J. Am. Chem. Soc. 136 (2014) 4394–4403.
[7] T.Y. Ma, J. Ran, S. Dai, M. Jaroniec, S.Z. Qiao, Phosphorus-doped graphitic carbon nitrides grown in situ on carbon-fiber paper: flexible and reversible oxygen electrodes, Angew Chem. Int. Ed. 54 (2015) 4646–4650.
[8] Mohd. Khalid, H. Varela, A general potentiodyamic approach for red phosphorous and sulfur nanodots incorporated on reduced graphene oxide sheets: metal-free and binder-free electrodes for supercapacitors and hydrogen evolution activities, J. Mater. Chem. A 6 (2018) 3141–3150.
[9] Mohd. Khalid, Ana M.B. Honorato, E.A. Ticianelli, H. Varela, Uniformly self-decorated Co3O4 nanoparticles on N, S co-doped carbon layers derived from a camphor sulfonic acid and metal-organic framework hybrid as an oxygen evolution electrocatalyst, J. Mater. Chem. A 6 (2018) 12106–12114.
[10] Q. Li, C. Yang, L. Wu, H. wang, X. Cui, Converting benzene into ϒ-graphyne and its enhanced electrochemical oxygen evolution performance, J. Mater. Chem. A 7 (2019) 5981–5990.
[11] J. Li, X. Gao, B. Liu, Q. Feng, X.-B. Li, M.-Y. Huang, Z. Liu, J. Zhang, C.-H. Tung, L.-Z. Wu, Graphdiyne: a metal-free material as hole transfer layer to fabricate quantum dot-sensitized photocathodes for hydrogen production, J. Am. Chem. Soc. 138 (2016) 3954–3957.
[12] P. Wu, P. Du, H. Zhang, C. Cai, Praphyne as a promising metal-free electrocatalyst for oxygen reduction reactions in acidic fuel cells, J. Phys. Chem. C 116 (2012) 20472–20479.
[13] Z. Zuo, H. Shang, Y. Chen, J. Li, H. Liu, Y. Li, Y. Li, A facile approach for graphdiyne preparation under atmosphere for an advanced battery anode, Chem. Comm. 53 (2017) 8074–8077.
[14] Q. Li, Y. Li, Y. Chen, L. Wu, C. yang, X. Cui, synthesis of ϒ-graphyne by mechanochemistry and its electronic structure, Carbon 136 (2018) 248–254.
[15] X. Kong, Y. Huang, Q. Liu, Graphyne nanosheet: a new metal-free catalyst for oxygen evolution reaction, Carbon 123 (2017) 558–564.
[16] F. Razmjooei, K. Singh, T.H. Kang, N. Chaudhari, J. Yuan, J.S. Yu, Urine to highly porous heteroatomdoped carbons for supercapacitor: a value added journey for human waste, Sci. Rept. 7 (2017) 10910.
[17] N.K. Chaudhari, M.Y. Song, J.S. Yu, Heteroatom-doped highly porous carbon from human urine, Sci Rept. 4 (2014) 5221.
[18] J.S. Lee, M.E. Briggs, C.C. Hu, A.I. Cooper, Controlling electric double-layer capacitance and pseudocapacitance in heteroatom-doped carbons derived from hypercrosslinked microporous polymers, Nano Energy 46 (2018) 277–289.
[19] Y. Deng, Y. Xie, K. Zou, X. Ji, Review on recent advances in nitrogen-doped carbons: preparations and applications in supercapacitors, J. Matr. Chem. A 4 (2016) 1144–1171.
[20] M. Biswal, A. Banerjee, M. Deo, S. Ogale, From dead leaves to high energy density supercapacitors, Ener. Environ. Sci. 6 (2013) 1249–1259.
[21] K. Krishnamoorthy, S.J. Kim, Mechanochemical preparation of graphene nanosheets and their supercapacitor applications, J. Ind. Eng. Chem. 32 (2015) 39–43.
[22] X. Huang, X. Zhou, Y. Meng, E. Mikmekova, H. Chen, D. Voiry, A. Goswami, M. Chhowalla, T. Asefa, Yeast cells-derived hollow core/shell heteroatom-doped carbon microparticles for sustainable electrocatalysis, ACS Appl. Mater. Interfaces 7 (2015) 1978–1986.
[23] M.A. Pimenta, G. Dresselhaus, M.S. Dresselhaus, L.G. Cancado, A. Jorio, R. Saito, Studying disorder in graphite-based systems by Raman spectroscopy, Phys. Chem. Chem. Phys. 9 (2007) 1276–1290.
[24] L. Zong, X. Yu, H. Yu, H. Xue, L. Feng, Nanostructured FeNi3 incorporated with carbon doped with multiple nonmetal elements for the oxygen evolution reaction, ChemSusChem 11 (2018) 2703–2709.
[25] Z. Liu, Y. Wang, L. Feng, A facile approach for constructing nitrogen-doped carbon layers over carbon nanotube surface for oxygen reduction reaction, J. Solid State Electrochemistry 22 (2018) 3467–3474.
[26] J. Sun, G. Zheng, H.-W. Lee, N. Liu, H. Wang, H. Yao, W. Yang, Y. Cui, Formation of stable phosphorus-carbon bond for enhanced performance in black phosphorus nanoparticle-graphite composite battery anodes, Nano Lett. 14 (2014) 4573–4580.
[27] G.-L. Tian, M.-Q. Zhao, D. Yu, X.-Y. Kong, J.-Q. Huang, Q. Zhang, F. Wei, Nitrogen-doped graphene/carbon nanotube hybrids: in situ formation on bifunctional catalysis and their superior electrocatalytic activity for oxygen evolution/reduction reaction, Small 10 (2015) 2251–2259.

[28] J.Q. Tian, Q. Liu, A.M. Asiri, K.A. Alamry, X.P. Sun, Ultrathin graphitic C3N4 nanosheets/graphene composites: efficient organic electrocatalyst for oxygen evolution reaction, ChemSusChem 7 (2014) 2125–2130.
[29] J. Lai, S. Li, F. Wu, M. Saqib, R. Luque, G. Xu, Unprecedented metal-free 3D porous carbonaceous electrodes for full water splitting, Ener. Env. Sci. 9 (2016) 1210–1214.
[30] K.G. Qu, Y. Zheng, S. Dai, S.Z. Qiao, Graphene oxide-polydopamine derived N, S-codoped carbon nanosheets as superior bifunctional electrocatalysts for oxygen reduction evolution, Nano Energy 19 (2016) 373–381.
[31] S. Chen, J.J. Duan, M. Jaroniec, S.Z. Qiao, Nitrogen and oxygen dual-doped carbon hydrogen film as a substarte-free electrode for highly efficient oxygen evolution reaction, Adv. Mater. 26 (2014) 2925–2930.
[32] R. Li, Z.D. Wei, X.L. Gou, Nitrogen and phosphorous dual-doped graphen/carbon nanosheets as bifunctional electrocatalysts for oxygen reduction and evolution, ACS Catal. 5 (2015) 4133–4142.
[33] N.Y. Cheng, Q. Liu, J.Q. tian, Y.R. Xue, A.M. Asiri, H.F. Jiang, Y.Q. Hee, X.P. Sun, Acidically oxidized carbon cloth: a novel metal-free oxygen evolution electrode with high catalytic activity, Chem. Comm. 51 (2015) 1616–1619.
[34] Y. Cheng, Y. Tian, X. Fan, J. Liu, C. Yan, Boron doped multi-walled carbon nanotubes as catalysts for oxygen reduction reaction and oxygen evolution reaction in alkaline media, Electrochim. Acta 143 (2014) 291–296.
[35] L. Dai, C. Hu, Multifunctional carbon-based metal-free electrocatalysts for simultaneous oxygen reduction, oxygen evolution, and hydrogen evolution, Adv. Mater. 29 (2017) 1604942.
[36] R.M. Yadav, J. Wu, R. Kochandra, L. Ma, C.S. Tiwari, L. Ge, G. Ye, R. Vajtai, J. Lou, P.M. Ajayan, Carbon nitrogen nanotubes as efficient bifunctional electrocatalysts for oxygen reduction and evolution reactions, ACS Appl. Mater. Interfaces 722 (2015) 11991–12000.
[37] X. Cai, L. Zhou, B. Tan, C. Yang, L. sun, Y. Wang, S. Zhou, Heteroato-doped carbon nanospheres derived from cuttlefish ink: a bifunctional electrocatalyst for oxygen reduction and evolution, Int. J. Hydr. Enr. 43 (2018) 17708–17717.
[38] T. Ying, X. Xiaoying, L. Wei, T.D. Ming, D. Kong, Z. Hong, N. Hirotoma, I. Takafumi, L. Baohua, D. Dmitiri, K. Feiyu, K. Takashi, Y.Q. Hong, Towards ultrahigh volumetric capacitance: graphene derived highly dense but porous carbons for supercapacitors, Sci. Rep. 3 (2013) 2975.
[39] S. Baskar, K. Ziyauddin, P. Seungyoung, K. Kyoungho, K. Hyunhyub, K. Youngsik, Highly porous graphitic carbon and $Ni_2P_2O_7$ for a high performance aqueous hybrid supercapacitor, J. Mater. Chem. A 3 (2015) 21553–21561.